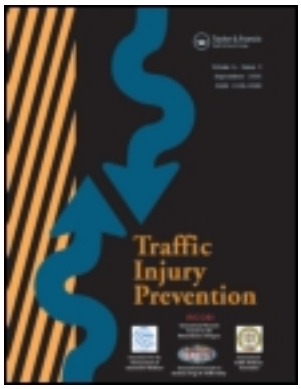

Traffic Injury Prevention
Publication details, including instructions for authors and subscription information:
http://www.tandfonline.com/loi/gcpi20

Pedestrian Lower Limb Injury Criteria Evaluation: A Finite Element Approach

P. J. Arnoux [a] , D. Cesari [b] , M. Behr [a] , L. Thollon [c] & C. Brunet [a]
[a] Laboratoire de Biomécanique Appliquée , Université de la Méditerranée , Marseille, France
[b] INRETS Scientific direction-Lyon , Bron, France
[c] MECALOG-Safety Business Unit , Paris, France
Published online: 25 Jan 2007.

To cite this article: P. J. Arnoux , D. Cesari , M. Behr , L. Thollon & C. Brunet (2005) Pedestrian Lower Limb Injury Criteria Evaluation: A Finite Element Approach, Traffic Injury Prevention, 6:3, 288-297, DOI: 10.1080/15389580590969463

To link to this article: http://dx.doi.org/10.1080/15389580590969463

Traffic Injury Prevention, 6:288–297, 2005

ISSN: 1538-9588 print / 1538-957X online
DOI: 10.1080/15389580590969463

Taylor & Francis
Taylor & Francis Group

Pedestrian Lower Limb Injury Criteria Evaluation: A Finite Element Approach

P. J. ARNOUX
Laboratoire de Biomécanique Appliquée, Université de la Méditerranée, Marseille, France

D. CESARI
INRETS Scientific direction-Lyon, Bron, France

M. BEHR
Laboratoire de Biomécanique Appliquée, Université de la Méditerranée, Marseille, France

L. THOLLON
MECALOG-Safety Business Unit, Paris, France

C. BRUNET
Laboratoire de Biomécanique Appliquée, Université de la Méditerranée, Marseille, France

Objective. *In pedestrian traumas, lower limb injuries occur under lateral shearing and bending at the knee joint level. One way to improve injury mechanisms description and consequently knee joint safety is to evaluate the ultimate shearing and bending levels at which ligaments start being injured.*

Methods. *As such data cannot easily and accurately be recorded clinically or during experiments, we show in this article how numerical simulation can be used to estimate such thresholds. This work was performed with the Lower Limb Model for Safety (LLMS) in pure lateral bending and shearing conditions, with an extended range of impact velocities.*

Results. *One result concerns the ultimate knee lateral bending angle and shearing displacement measurements for potential failure of ligaments (posterior cruciate, medial collateral, anterior cruciates and tibial collateral). They were evaluated to be close to 16° and 15 mm, respectively.*

Conclusion. *The lower leg model used in this study is an advanced FE model of the lower limb, validated under various situations. Its accurate anatomical description allows a wide range of applications. According to the validity domain of the model, it offered a valuable tool for the numerical evaluation of potential injuries and the definition of injury risk criterion for knee joint.*

Keywords Transportation; Biomechanics; Finite Element Method; Injury Probability; Pedestrians; Legs

Safety concerns have been taking a large and increasing place in the car design process. The assessment of car crashworthiness is more and more related to the evaluation of injury risk for car occupants, pedestrians, and cyclists, and the development of advanced safety systems. At a research level, the first point of interest is injury mechanisms. This is why both experimental and numerical approaches have been used to investigate the human behavior and tolerance under impacts and to develop realistic human body models (Nyquist et al., 1985; Kajzer et al., 1993; Crandall et al., 1996; Parenteau, 1996; Atkinson et al., 1998; Lizee et al., 1998; Arnoux et al., 2001; Beillas et al., 2001; Thollon et al., 2001; Behr et al., 2003).

Received 26 July 2004; accepted 14 March 2005.

Address correspondence to P. J. Arnoux, Laboratoire de Biomécanique Appliquée, UMRT 24 Faculté de Médecine-INRETS, Université de la Méditerranée, Marseille, France. E-mail: pierre-jean.arnoux@inrets.fr

PEDESTRIAN BIOMECHANICS

In the field of pedestrian injury biomechanics, lower limbs are highly loaded during crash situations (AIS from 2 to 6) with joints damages and bones failures (Stutts et al., 1999; IHRA 2000). From an experimental point of view, during a pedestrian impact, knee injuries could be produced by a combination of lateral shearing and bending of the knee (Kajzer et al., 1990, 1993; Grzegorz et al., 2001; Bose et al., 2004). On cadaver full leg experiments, Kajzer et al. (1990, 1993) focused on impact forces and bending moments corridors. They showed that pure shearing induces collateral tibial and anterior cruciate ligament

failure while a primarily bending mainly induces medial collateral ligament failure. More recently, Bose et al. (2004) worked on 3-point bending tests on isolated knee joints in order to obtain a combination of shearing and bending effects, and confirmed injuries to medial collateral and anterior cruciate ligaments. Knee injuries are not restricted to the injuries described above. Tibia fractures (especially the tibial eminence in contact with the intercondylar notch at impact), PCL injuries, and fibula and femur fractures can also be observed. From all these studies, it appears that the main challenge for improving leg protection should focus on knee ligament damage and failure minimization.

ABOUT NUMERICAL MODELS

Numerical simulation and, more specifically, finite element modelling can be very helpful to complete injury mechanisms understanding, once the finite element model is validated through appropriated experimental tests. Many finite element models have been designed to study very specific points of the leg behavior under crash situations. The ankle-foot models (Beaugonin et al., 1996, 1997; Tannous et al., 1996; Beillas et al., 1999) focus on structure behavior in inversion, eversion, dorsiflexion, and response under axial loading. Knee models were also developed for frontal impacts (Hayashi et al., 1996; Atkinson, 1998; Atkinson et al., 1998) or pedestrians (Yang et al., 1997; Schuster et al., 2000). Lastly, (Bedewi et al., 1996) included mathematical joints to control the kinematics of a full lower limb model. More recently, accurate finite element models of the whole lower limb were designed to investigate joints traumas during crash situations, especially for pedestrian applications (Schuster et al., 2000; Takahashi et al., 2003). The LLMS model used in this study, jointly developed by MECALOG and the Laboratory of Biomechanics and Applications, and in association with the Wayne State University, was based on an accurate description of all anatomical parts of the lower limb. Its validation (on isolated materials levels, sub-segment levels up to the whole model level) was performed in many different impact situations (Arnoux et al., 2001, 2002b, 2003, 2004; Beillas et al., 2001). This model was designed, improved, and used in the Radioss non-linear FE code environment.

Usually, numerical model validation compares responses obtained from simulations using the finite element model with experimental test results performed under the same impact conditions. One major interest in human modelling lies in the possibility of numerically recording specific parameters (strain, stress, pressures, and kinematics) that could not be available during experiments. With this data, it becomes easier to show tissue kinematics and mechanical behavior during the crash chronology and then, to postulate on potential injuries. For knee injuries on pedestrians, one way to define an injury risk criterion or an injury probability for knee soft tissues is to evaluate the ultimate lateral bending and shearing levels of the knee before damage, when the impact occurs. To investigate the corresponding injury mechanisms and then evaluate these ultimate levels, we have used the last version of the LLMS finite element model of the lower limb.

OBJECTIVES

This article focuses on the evaluation of injury criteria for the knee ligaments regarding lateral impact situations of an isolated limb. The work consisted in analyzing the model response looking for a relationship between bone Von Mises stress levels, ligaments global and local strain levels, and kinematics information such as knee rotation and shearing measurements. These numerical simulations are based on previous experimental work reported by Kajzer et al. (1990, 1993), that is, lateral bending impact tests on an isolated lower limb (the impact being applied on the internal malleolus), and pure shearing impact tests on an isolated lower limb, the tibia being loaded simultaneously at its two extremities. As impact velocity in pedestrian is a gravity factor, this first test campaign focused on extended velocities ranging from 2 to 10 m/s. Prior to this analysis, a summary of the model design and validation steps, already described in detail in Arnoux et al. (2001, 2002, 2003, 2004), Beillas et al. (2001), is given.

MODEL OVERVIEW: FROM DESIGN TO VALIDATION

Model Geometry

The model geometry was obtained through MRI measurements on a 50th percentile human male volunteer. Measurements were performed in the sagittal plane from the hip to the toe region (the leg being extended). The scanning step was of 1 mm in joint regions and ranged from 5 mm to 10 mm in other parts. Moreover, longitudinal and frontal scans taken between the femur and tibia were used to complete the geometry acquisition. Once MRI measurements were achieved, anatomical components were identified on each section. The contours were then computed to create a 3D reconstruction of the lower limb. It was then possible to mesh all parts of the model using shells, bricks, or springs depending on the modeled part. The characteristic lengths were defined to settle an initial time step of 0.8 to 1 μs. In the version used in this study, the model includes 25298 nodes (13567 shells, 11145 solids, 503 springs) gathered in 162 different mechanical parts. The current model includes compact and trabecular bones, knee cartilages, menisci, knee ligaments, tendons, and skin as well as a simplified muscle description.

Modeling Task

Because of the cortical bones thickness and the time step constraint, compact bones were modeled using shell elements. The inner and outer cortical surfaces were used to compute a midsurface and to estimate the bone local thickness at the different levels of the bones. The bones were divided in several geometrical parts in order to take bone thickness and density distribution into account. The spongious bone of femur, patella, tibia, fibula, talus, and calcaneum were meshed with solid elements. Solid elements and their surrounding shells were not coincident, but connected using tied contact interfaces. Compact and spongious bones were modeled with a Johnson Cook elasto-plastic material law. According to the literature data, it is established that material and geometrical properties of biological tissues (bones in particular) changes according to the considered region. These

Table I Summary of elastoplastic properties of bones

	Compact	Spongious
Young modulus	9–15 Gpa	10–450 Mpa
Poisson ratio	0,3	0,3
Yield stress	80–120 Mpa	10 MPa
Ultimate stress	110–130 Mpa	15 MPa
Hardening (param & coef)	100 Mpa, 0,1	100 Mpa, 0,1
Ultimate strain	2–3%	3%

continuous changes from epiphysis to diaphysis were included in the model regarding density, thickness and Young's modulus.

Foot bones (the 5 metatarsis, the 5 phalanx, the 3 cuneiforms, and the cuboid) were set rigid. Mechanical parameters of bones (McElhaney et al., 1966; Burstein et al., 1972; Reilly et al., 1975; Goldstein et al., 1987) are summarized in Table I. Foot and ankle ligaments were modeled using either elastic springs or viscoelastic shells. When springs were used, each ligament was defined as a bundle of spring elements in order to improve interactions modeling (i.e., contact interfaces) between ligaments and bones. The same method was used for the Achilles tendon. Knee soft tissues were modeled using bricks, shells, or springs elements, depending on the dimensions of the corresponding tissue. Cruciate ligaments and patellar tendon were described using both solids and shells in order to model membranes around the structure. Low stiffness springs were also added to compute deformations on the ligament using gauges with length ranging from 2 to 5 mm along the main axes of the ligament. Lateral ligaments and patellar wings were described using shell elements. Lastly, fibular-tibial ligaments and meniscus ligaments were described using springs.

Ligaments and tendons of the knee were modeled with a generalized viscoelastic Kelvin Voigt material law or using elastic or viscoelastic springs based on literature data (Arnoux, 2000; Johnson, 1996; Noyes, 1976; Attarian et al., 1985) (Table II). Cartilage and menisci, which contribute to an accurate control and a good stability of the knee during its movement, were modeled using elastic solid elements. This biphasic material (incompressible fluid within a fibrous structure) is highly strain rate dependent and mechanical properties of such a structure are strongly linked to fluid exudation effects during loading. In this study, as the material was assumed to be elastic, we chose a high Young's modulus value (20 MPa) in order to take into account strain rate influence under dynamic loadings (Yamada, 1970; Repo et al., 1977; Atkinson, 1998). Same assumptions were formulated for meniscus with a Young modulus of 200 MPa, also considering the structural differences with cartilages (Radin et al., 1970; Yamada, 1970; Mow et al., 1992; Li et al., 2003).

Table II Summary of viscoelastic properties of ligaments

	Ligaments & tendons
Young modulus	50–225 Mpa
Poisson ratio	0,3
Tengent Young modulus	48–155 Mpa
Tengent Poisson ratio	0,37
Viscosity in pure shear	6,6

Because of the lack of data on its dynamic properties, the capsula was described as an elastic material using shell elements (with a Young's modulus of 20 MPa). Muscles were modeled in two separate ways. Firstly, muscles action lines are described using springs elements (not active in the current model). They also include solid elements in order to give a unique volumic shape to muscles and other aponevrotic tissues. Note that muscles were assumed as elastic materials at this stage. Except for the foot phalanx joint described with a mathematical joint, all joints are defined using all anatomical components that contribute to joint kinematics and stability. Therefore, and in order to ensure interaction between tissues, several interfaces were defined:

1. Bones to bones, bones to ligaments, and ligaments to ligaments. Cartilages to cartilage interfaces are used to describe joints or moving tissue contacts. They are modeled using self contact interfaces and edge to edge contact interfaces.
2. Tied contact interfaces, which ensure attachments (spongious bone to compact bone, flesh to bones), were modeled.

Model Validation

The model validation focused on mechanical properties of tissues, model ability to describe passive physiological movements, sub-segment behavior under specific loading and finally, whole model testing (cf. validation database summary in Table III). To

Table III Summary of model validation database

	Computed data	Reference
Isolated material		
Anterior cruciate traction	Force, Displacement	Arnoux, 2000
Posterior cruciate traction	Force, Displacement	Arnoux, 2000
Medial collateral liagment traction	Force,Displacement	Arnoux, 2000
Tibial collateral liagment traction	Force, Displacement	Arnoux, 2000
Three point femur bending	Force, Displacement	Beillas, 1999
Patellar tendon traction	Stress, Strain	Johnson, 1996
Sub-segment tests		
Knee joint kinematic		
Haut patellar impact on flexd knee	Force, time	Haut, 1995
Hayashi patellar impact on flexed knee	Force, time	Hayashi, 1996
Banglmeier tibia impact on flexed knee	Force, time	Banglmeier, 1999
Antero-posterior flexed knee loading	Force, Displacement	Viano, 1978
Tibia latero-medial 3 point bending	Force, time	Nyquist, 1985
Tibia antero-posterior 3 point bending	Force, time	Nyquist, 1985
Quasi-static lower leg compression	Force, displacement	Bennet, 1990
Quasi-static tibo-fibular compression	Force, displacement	Beillas, 2001
Ankle inversion	Moment, rotation	Parenteau, 1996
Ankle eversion	Moment, rotation	Parenteau, 1996
Ankle dorsiflexion	Moment, rotation	Parenteau, 1996
Whole LLMS model		
Pedestrian LBA lateral bending	Force, Rotation	Kajzer, 1993
Pedestrian LBA lateral shearing	Force, time	Kajzer, 1990
Frontal Wayne sled test	Force, time	Beillas, 2001

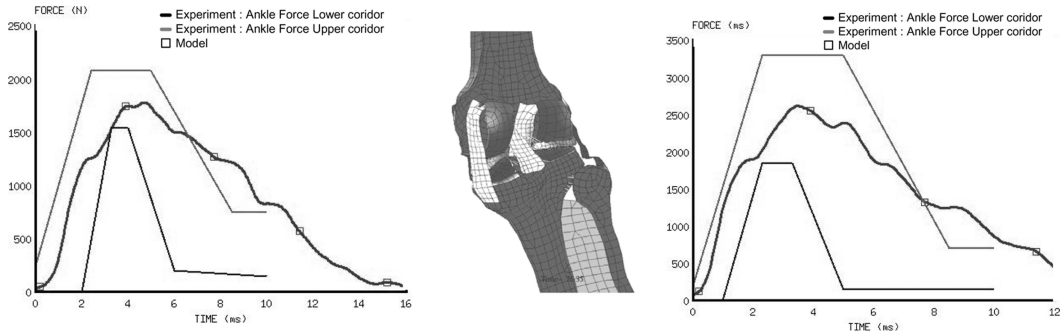

Figure 1 Von Mises stress curves on knee ligaments and on lower limbs bones. Lastly force vs. time curve for 16 and 20 km/h impact velocity on the ankle impactor.

give an overview of the model validation, example of validation tests are reported below.

1. The mechanical properties of isolated tissues were checked under traction tests on isolated knee ligaments with a constant velocity of 1.98 m/s (Arnoux et al., 2002a). Parameters identification was based on previously estimated parameters (Arnoux, 2000) coupled with optimization procedures using the Radioss DSS optimizer tool. Note that failure properties were not integrated. During the loading test, it was also possible to show stress distribution in the ligaments structure. Localization of high stress levels in the neighbouring of bone insertion can be compared (in terms of location) with failure profiles observed during the experimental tests.
2. The second level was illustrated with the model ability to describe knee passive flexion (gravity loading). Kinematics were checked by anatomists focusing on the combined sliding and rolling movement of the femur on the proximal tibia. The sliding of the patella between the two femoral condyles and the action of the ligaments linked to the patella were checked. The interaction between the two cruciate ligaments during flexion and, at last, the contribution of meniscus to ensure a correct contact interface between bones were also checked. Note that a recent model improvement including a separate modelling of muscles with their active behavior (Behr, 2003) shows the same behavior with muscle tonicity.
3. The third validation level deals with sub segment testing in order to evaluate the structure behavior including soft and hard tissues. For the sub segment validation testing (Table III), model validation was obtained by comparison with experiments of Force versus Time, Force versus Deflexion, and Moment versus Rotation curves.
4. The full model validation was obtained by frontal and lateral crash situations to identify complete injury mechanisms. The lateral bending impact test was performed to identify one of the main injury mechanism occurring in pedestrian impacts (Kajzer et al., 1990, 1993). In these experimental tests, the upper leg was allowed to freely translate in the vertical direction, while a 22 kg dead weight was attached to the proximal femur to simulate the body weight. The foot was placed on a plate to allow free translation along the direction of impact. A 40 kg impactor was used to load the distal tibia at an impact velocity of 16 and 20 Kph. The model validation was performed by comparing forces versus time recorded on the impactor face. Results were found within the experimental corridors (Figure 1).

For the shearing tests, the impactor had two impacting surfaces simultaneously applied on both proximal and distal extremities of fibula and tibia (Figure 2). The knee impact force versus time curve revealed two different injury mechanisms. The first injury mechanism which can be directly related to the knee impact force (for example head of fibula failure, or extra articular fracture) occurred approximately 5 ms after the contact and was identified as the first peak on the force versus displacement curve. The second injury mechanism was correlated to the force transmitted through the knee joint during the

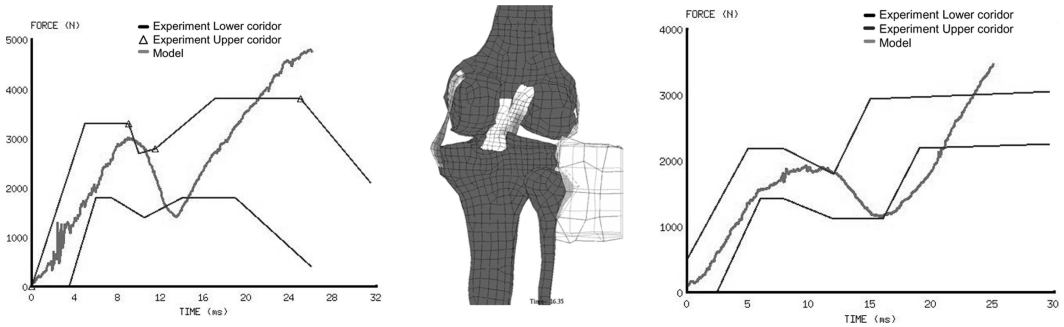

Figure 2 Von Mises stress curves on lower limbs knee ligaments and on bones. Lastly force vs. time curve for 16 and 20 km/h impact velocity on the ankle impactor.

impact. This phenomenon was identified by the relative displacement of the tibia which produces injuries in the neighbouring ligaments. The resulting impacting forces predicted by the leg model were not fully relevant with the experimental corridor (Figure 2). The two-stage injury mechanism experimentally identified, with the two peaks in the force time curve, was not reproduced with the LLMS model. In the case of a shearing impact, the injury mechanism is very complex and follows two steps.

The first injury mechanism (occurring 5 ms after impact), is directly related to the knee impact force. It can be described as a contact injury and can induce bone fractures (head of fibula, tibia or femur). The second injury mechanism is correlated to forces transferred through the knee during acceleration of the thigh (relative shearing of tibia versus femur), which lead to soft tissues injuries. This could be linked to soft tissue behavior laws as physical failure was not implemented in the model. However, the locations of stress concentrations predicted by the model, including the cruciate ligament insertions, the tibia eminence and the tibia fibular joint, were in agreement with the injury locations found during the necropsies (Figure 2). For these two tests, the deformation levels were recorded on each ligament and used to postulate on potential injuries. This point is detailed hereafter.

LIGAMENTS INJURY PROBABILITY EVALUATION

Methodology Overview

As it is possible to compute data not usually recordable experimentally, such as stress distribution, strain levels, pressure or specific displacements, the finite element simulation was used to focus on the impact chronology. Usually (Tropiano et al., 2004; Thollon et al., 2003), when coupling mechanical analysis and medical interpretation, numerical injury identification is assessed through the analysis and the interpretation of the parameters discussed hereafter.

For this work the numerical experiments consisted first in lateral bending impact tests on an isolated lower limb (the impact being applied on the internal malleolus). Then, a pure shearing impact test on an isolated lower limb was performed (the tibia being loaded simultaneously at its two extremities). The test campaign was extended to velocities ranging from 2 to 10 m/s.

Kinematics Interpretation. Kinematics is recorded in order to check the global behavior of the model and to study interactions with the environment. In the LLMS model, these kinematics can also be recorded at each joint in order to check the correct relative movements between the corresponding bones or soft tissues. It gives, in a first approximation, information about the global kinematics behavior (in lateral bending, in flexion-extension, in rotation, or during combined motions) to validate the correct function of joints. In this work, we specifically focused on the relative rotation between tibia and femur. By computing the scalar product between femoral and tibial axes (frontal and antero-posterior), it was possible to calculate knee torsion, lateral bending and frontal bending in the different planes and for each test. Therefore, concerning shearing, the lateral relative displacement between the tibial eminence and the intercondylar notch was calculated to accurately identify knee lateral shearing in the joint.

The Force and Stress Level. The force, and more particularly the stress level and distribution in bones (against time), can be studied to evaluate the location and evolution of hard tissue injuries. Due to the mechanical properties of bones, damage is assumed to occur on bone structure when stress reaches the Yield stress values. The different Von Mises stress levels obtained in the model are compared to the Yield and ultimate stress level implemented in the different sets of parameters of the compact bone.

Strain Measurements. Can be mainly attributed to soft tissue injury evaluation. Damage properties of soft tissues can be described in terms of ultimate strain level in soft tissue structures. In the particular case of the knee ligaments, previous experimental work (Arnoux et al., 2000, 2002a) produced the mechanical properties of knee ligaments under dynamic loadings, up to complete failure of the structures. The results led to consider ligament failure with a strain criterion. Ultimate strain levels were calculated for the four knee ligaments and used in this study to identify potential failure. Note that literature gives various values for ultimate strain (Table IV) obtained in different experimental conditions (e.g., loading, preconditioning, conservation).

For each of the four knee ligaments, strain sensors were inserted in the model. These sensors consist in a series of springs along the main fiber axes of the ligaments, each spring having a stiffness set to zero. For the cruciate and lateral ligaments, it was also possible to calculate the global strain level, the average strain level as well as the curve of maximum strain recorded at various levels in the ligament. These calculated strain levels are then compared to the experimental ultimate strain levels (Table IV) to postulate on a potential failure of the ligaments during the test. The same experiments as those described in the model validation chapter were used. The impact velocities chosen for these studies are 2 m/s, 4 m/s, 5.55 m/s, 7 m/s and 10 m/s. The typical impact force recorded on the impactor during each test (and reported in Figure 3) gives an overview of the velocity influence on numerical simulations.

Table IV Overview of ultimate strain levels recorded for knee ligaments

Author	Collateral tibial	Collateral medial	Posterior cruciate	Anterior cruciate
Viidick, 1973	30%	40%	60%	60%
Kennedy, 1976			24 (±6)%	
Marinozzi, 1982			20 (±5)%	
Prietto, 1992			28 (±9)%	
Race, 1994			18 (±5)	
Arnoux, 2000	24–38%	22–38%	15–23%	18–24%
Kerrigan, 2003	7–10%	11–20%		

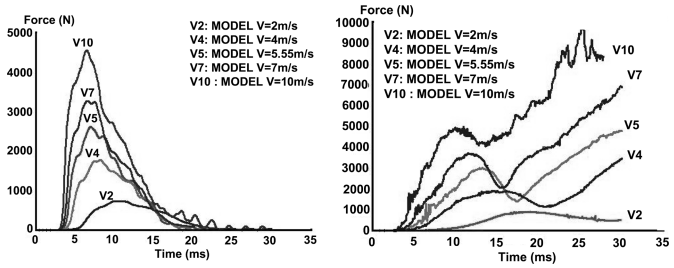

Figure 3 Unshifted impact forces recorded on medial ankle versus time for the five impacts velocities in bending test. Impact force recorded on the upper bumper during the shearing test.

Forces and Stress Analysis

The Von Mises stress levels on bones were located on the proximal tibial metaphysis and distal femoral metaphysis (Figure 4) for both impact situations. For bending tests, the maximum Von Mises stress level stays lower than the failure level and reaches 30 MPa at 2 m/s, 60 MPa at 4 m/s, 70 MPa at 5.55 m/s, 90 MPa at 7 m/s, and 125 MPa at 10 m/s (which is close to the limit of failure). Note that stress concentration was also observed on ligament insertions (with lower values than those reported upwards). For shearing tests, the bones Von Mises levels are higher. They reach 60 MPa at 2 m/s, 93 MPa at 4 m/s, 115 MPa at 5.55 m/s, 120 MPa at 7 m/s and 130 MPa at 10 m/s (with tibia failure). Stress concentrations were observed at the contact area between proximal fibula and tibia (and may be produced by the contact with the impactor), at the tibial eminence in contact with the intercondylar notch and at lower levels on ligaments insertions.

Kinematics Aspects

For bending tests, the typical lateral rotation between the tibia and the femur was recorded with a rotation axis that seems to pass through the contact area between the femoral external condyle and the tibial external glena. The frontal rotation is stable with a variation ranging from 1° to 3°, depending on the impact velocity. The torsion effect seems to be important and correlated to the impact velocity (Figure 5). Variation of angles reaches

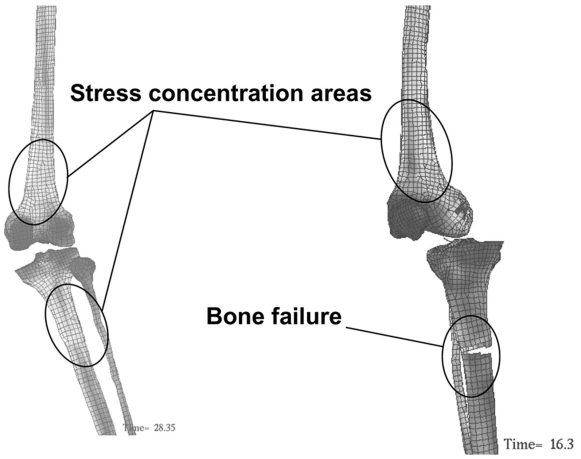

Figure 4 Von Mises stress on bones for bending ($V_0 = 5.55$ m/s) and shearing impact ($V_0 = 10$ m/s).

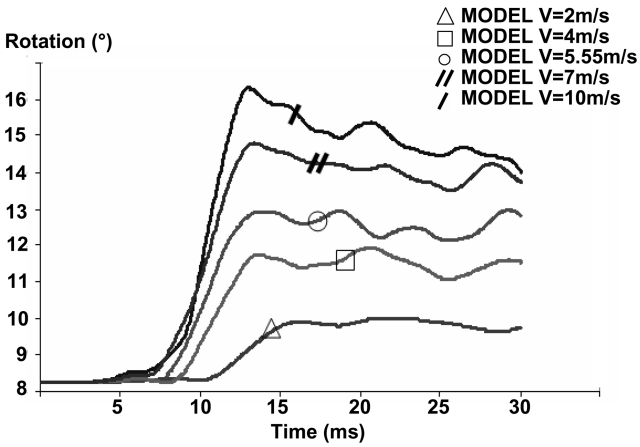

Figure 5 Bending case: Knee torsion versus time.

values ranging from 2° to 8°, depending on the impact velocity. This point has to be linked to the asymmetrical geometry of the femoral condyle and the tibial glena. From a medical point of view, this torsion effect is described as a natural safety countermeasure of the human body during trauma situations to avoid (or limit) damage to ligaments. Lastly, lateral shearing effects could be neglected for this test.

For shearing tests, the two main kinematics aspects are the lateral shearing and the knee torsion. The lateral shearing seems to be correlated with velocity and rapidly reaches strong values. In the first 15 ms, the knee torsion reaches amplitudes ranging from 2° to 10° depending on the impact velocity.

Ligament Deflexion

Strain level recorded on each ligament (cruciate and lateral) and correlated to rotation effects were computed in two ways:

1. The total strain in the ligaments is obtained by summing up the deflexions recorded at each level of the ligament. This gives a general overview of the global strain on the structure.
2. The maximum strain in the ligaments is obtained with the maximum strain recorded at the different levels of the ligament. This strain gauge is used to locate high strain levels in the structure which could lead to damage or failure.

As previously mentioned, the implemented soft tissue behavior laws do not take into account damage and failure mechanisms. To postulate on damage in the structure, our analysis was based on strain levels recorded on the ligaments and compared to ultimate strain level at failure reported in a previously published experimental studies (Arnoux et al., 2002, 2003). In the present study, the ultimate values used to postulate on damage were assumed to be 28% for lateral ligaments, and 22% for cruciate ligaments. Then, maximum strain can be considered as a first sensor to locate damage in the structure whereas the total strain gives a global overview of the whole structure. If the maximum strain reaches the ultimate strain level as defined above, we assume that damage can occur in the ligament. Moreover, if

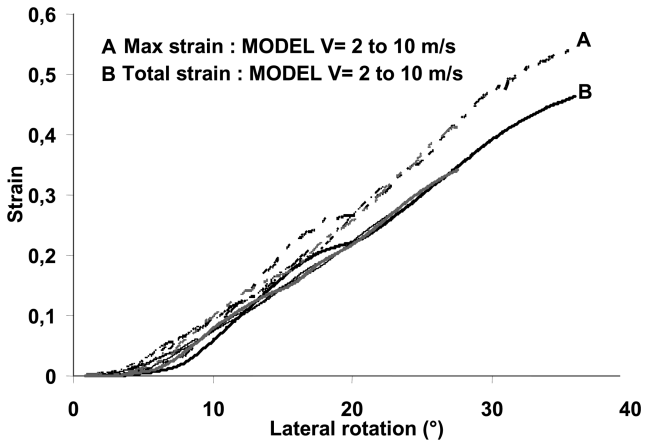

Figure 6 Bending case: Collateral medial ligament maximum strain versus lateral rotation.

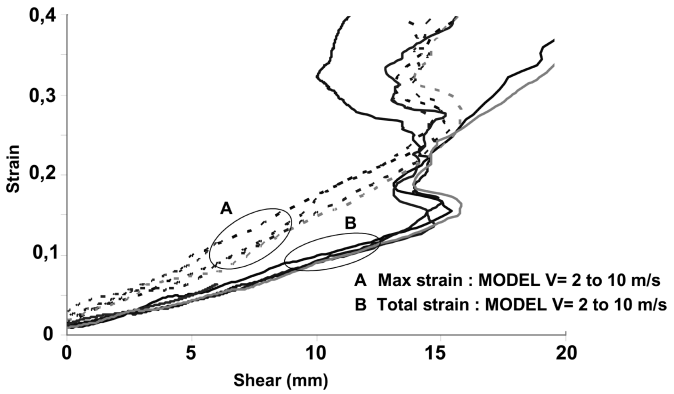

Figure 8 Shearing case: Anterior cruciate ligament maximum strain versus lateral shearing.

the ultimate strain level is reached on the total strain curve, the ligament failure can be postulated with a high probability.

For lateral bending tests, the lateral medial and the posterior cruciate ligaments were highly loaded (Figures 6 and 7). If the strain versus time curve shows a strong sensitivity to impact velocity, on the opposite, strain versus lateral bending seems to be independent of impact velocity (Figures 6 and 7). A small difference between maximum strain level and total strain level could indicate that the medial collateral ligament in the model has homogeneous strain distribution. The maximum strain or total strain level used to postulate on damage in the ligaments is obtained with a lateral rotation ranging from 20° to 24°. Concerning the posterior cruciate ligament, there is a strong difference between global strain (maximum strain) and local strain (maximum strain), which seems to show that local high strain levels were obtained. Local damage could occur for a knee rotation between 12° and 15°, whereas global damage for knee lateral rotations was close to 26° (which seems to be very high).

For the shearing tests, the two cruciate and the tibial collateral ligaments were highly loaded (Figures 8–10). As was observed in bending tests, the effects of impact velocity were significant on strain versus time curves and had no effects on strain versus knee shearing curves. The small dispersion observed between total strain and maximum strain seems to indicate that strain is homogeneous in the anterior cruciate ligaments. The failure or damage could start at a 13 to 15 mm knee shearing. For the posterior cruciate ligament, the strain being not homogeneous on the structure, only maximum strain levels were computed, and showed that damage could occur for shear values ranging from 12 to 14 mm. Finally, for the collateral tibial ligament, the maximum strain reaches up to 14-17 mm according to the impact velocity.

DISCUSSION

The objective of this work was to show how it is possible, when using FE model of the lower limb and numerical simulations at various impact velocities, to improve injury mechanism knowledge and to evaluate ultimate bending and shearing levels. Results illustrate the ability of the model to describe such impact situations and then provide a first estimation of these injury thresholds unavailable experimentally.

The LLMS Model

The LLMS model was first designed to provide a complete model of the lower limb that is validated under various impact situations in order to be able to work all the same in frontal impacts, pedestrian impacts or sports traumatology. From its initial version and according to its use, improvements were performed concerning

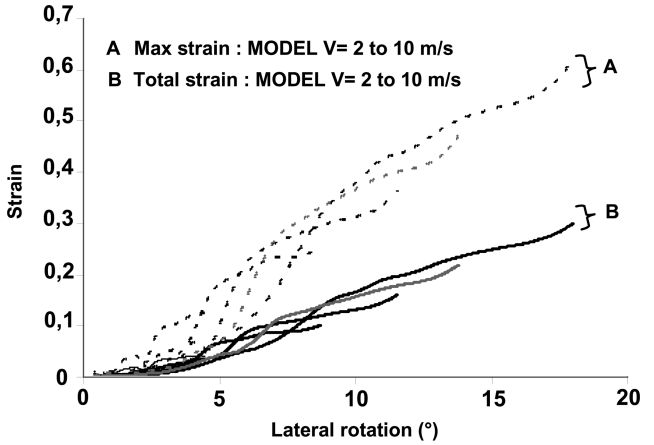

Figure 7 Bending case: Posterior cruciate ligament maximum strain versus lateral rotation.

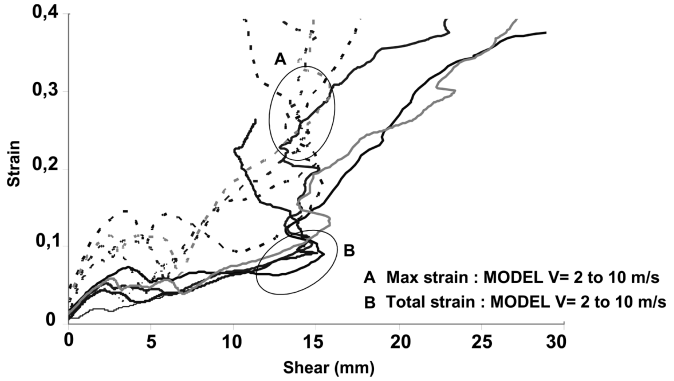

Figure 9 Shearing case: Posterior cruciate ligament maximum strain versus lateral shearing.

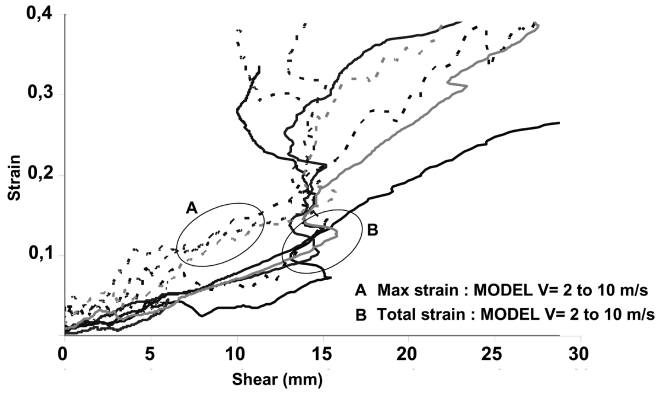

Figure 10 Shearing case: Collateral tibial ligament maximum strain versus lateral shearing.

mesh parts (meniscus, ankle and foot ligaments, flesh, muscles, pelvis), properties (bones Young modulus, muscles tone [Behr, 2004], joint definitions), interactions definitions and lastly validation database extension and update.

Regarding the model response (for example in the case of shearing tests), new improvements are necessary. It is now essential to include a damage model and a symmetric behavior for tissues, but also to include more precise material properties for biological tissues (e.g., cartilages, capsula, menisci, ankle ligaments). Lastly, criteria evaluated in this study should be improved by performing sensitivity studies in order to define a risk corridor for these ultimate levels.

Injury Criteria Evaluation

For the bending test, the knee injury mechanism can be described as a lateral rotation around the contact area between the lateral femoral condyle and the tibial glena. This rotation simultaneously induces a high deflection of both anterior cruciate and medial collateral ligaments, which were assumed to be injured for rotations of 15 and 20°, respectively. These results were not sensitive to impact velocities, and seem to be relevant with those experimentally identified at specific velocities.

For pure shearing impacts, the chronology of ligament failure concerned the anterior, posterior cruciate, and tibial collateral ligaments. The ultimate shearing level was computed by measuring the distance between the tibial eminence and the condylar notch that reached up to 13 to 15 mm. For both impact situations, the strain versus time curves showed the influence of impact velocity and the time dependent answer of the whole structure which could be mainly attributed to soft tissue viscoelastic properties. Concerning the kinematics aspects, whereas frontal flexion of the knee did not change significantly, torsion effects cannot be neglected, especially during the first phase of the impacts. This rotation, which could be attributed to the dissymmetry of the femoral condyles, was described as a safety countermeasure of the knee to avoid or limit ligament damage.

About Model Limits

As the model did not properly include damage behavior, its response validity has to be bound to the first ligament failure. This was illustrated by the response under shearing impact because strain levels recorded on ligaments were higher than ultimate values. As our objective was to focus on the bending or shearing level up to the first occurring ligament injury, the model response regarding to experimental corridors has to be compared in that sense. Nevertheless, it was observed that ultimate strain levels recorded in the ligaments reached their ultimate value much faster. Concerning bone modelling, bone failure was simulated by deleting elements once ultimate strain was reach. This point put limitation in the analysis of the bone failure phenomena and has to be improved including a damage and failure model.

Damping properties of muscles, which are significative in impact situations (Dhaliwal et al., 2002) were not implemented in the current model. However, as in Kajzer's tests (Kajzer et al., 1990, 1991, 1992, 1993) impacts regions were located on the internal malleola (for bending test) and simultaneously on the external malleola and fibular eminence for shearing tests, the flesh thickness was very thin compared to other regions, and should therefore not significantly modify our model response. This point has to be improved in further works.

Concerning ligaments structure, strain rate levels reach 10000%/s in the higher speed impact test. These strain rate levels are relevant to those used in previous experiments (Arnoux et al., 2000) which ranged from 5000 to 10000%/s according to the considered ligament. As these tests were used in the model validation, we can assume the model to be in the validity domain for the different tested impact velocities.

SUMMARY

The lower leg model used in this study is an advanced FE model of the lower limb, validated under various situations (from physiological movements up to frontal and lateral impacts). Its accurate anatomical description allows a wide range of applications. According to the validity domain of the model, it offered a valuable tool for the numerical evaluation of an injury risk criterion for knee soft tissues, through an ultimate bending of 15–20° and a shearing of 13–15 mm.

REFERENCES

Arnoux PJ, (2000) Modélisation des ligaments des membres porteurs. PhD dissertation. Université de la Méditerranée, Marseille, France.

Arnoux PJ, Cavallero C, Chabrand P, Brunet C. (2002a) Knee ligaments failure under dynamic loadings. *International Journal of Crashworthiness*, Vol.7, No. 3, pp. 255–268.

Arnoux PJ, Cesari D, Behr M, Thollon L, Brunet C. (2004) Pedestrian lower limb injury criteria evaluation a finite element approach, Proceedings of IRCOBI Conference, pp. 193–206.

Arnoux PJ, Kang HS, Kayvantash K. (2001) The Radioss human model for safety. *Archives of Physiology and Biochemistry*, Vol. 109, pp. 109.

Arnoux PJ, Kang HS, Kayvantash K, Brunet C, Cavallero C, Beillas P, Yang H. (2001) The Radioss Lower Limb Model for Safety: Application to lateral impacts. International Radioss User Conference. Sophia, Bulgaria.

Arnoux PJ, Thollon L, Behr M, Kayvantash K, Cavallero C, Brunet C. (2003) Advanced lower limb finite element model for human tolerance evaluation, IX International Symposium on Computer Simulation in Biomechanics, Sydney, Australia, pp. 13–21.

Arnoux PJ, Thollon L, Kayvantash K, Behr M, Cavallero C, Brunet C. (2002b) Advanced lower limb model with Radioss, application to frontal and lateral impact Radios lower limb model for safety, Proceedings of the IRCOBI Conference, pp. 373–375.

Atkinson P. (1998) A stress based damage criterion to predict articular joint injury from sub fracture insult. PhD dissertation. Michigan State University, East Lansing, MI.

Atkinson PJ, Haut R, Eusebi C, Maripudi V, Hill T, Sambatur K. (1998) Development of injury criteria for human surrogates to address current trends in knee-to-instrument panel injury, Stapp Car Crash Conference Proceedings, pp. 13–28.

Attarian DE, McCrackin HJ, McElhaney JH, DeVito DP, Garrett WE. (1985) Biomechanics characteristics of the human ankle ligaments. *Foot and Ankle*, Vol. 6, No. 2, pp. 54–58.

Banglmaier RF, Dvoracek-Driskna D, Oniang'o TE, Haut RC. (1999) Axial compressive load response of the 90 degrees flexed human tibiofemoral joint. 43rd Stapp Car Crash Conf. Proceedings, pp. 127–138.

Beaugonin M, Haug E, Cesari D. (1996) A numerical model of the human ankle/foot under impact loading in inversion and eversion. 40th Stapp Car Crash Conference Proceedings, pp. 239–249.

Beaugonin M, Haug E, Cesari D. (1997), Improvement of numerical ankle/foot model: Modeling of deformable bone. 41th Stapp Car Crash Conference Proceedings, pp. 225–237.

Bedewi PG, Bedewi NE. (1996) Modelling of occupant biomechanics with emphasis on the analysis of lower extremitiey injuries. *International Journal of Crash*, Vol. 1, pp. 50–72.

Behr M. (2004) Description et modélisation du comportement musculaire des membres pelviens–application à la sécurité routière, PhD dissertation, Marseille France.

Behr M, Arnoux PJ, Serre T, Bidal S, Kang HS, Thollon L, Cavallero C, Kayvantash K, Brunet C. (2003) A Human model for Road Safety. From geometrical acquisition to Model Validation with Radioss. International Journal on Computer Methods in Biomechanics and Biomedical Engineering, Vol. 6, No. 4, pp. 263–275.

Behr M, Arnoux PJ, Thollon L, Serre T, Cavallero C, Brunet C. (2003) Towards integration of muscle tone in lower limbs subjectes to impacts. IX International Symposium on Computer Simulation in Biomechanics, pp. 23–30.

Beillas P. (1999) Modélisation des membres inférieurs en situation de choc automobile, PhD dissertation, École Nationale Supérieure d'Arts et Métiers, Paris, France.

Beillas P, Arnoux PJ, Brunet C, Begeman P, Cavallero C, Yang K, King A, Kang HS, Kayvantash K, Prasad P. (2001) Lower limb: Advanced FE Model and new experimental data. *International Journal of STAPP—ASME*, Vol. 45, pp. 469–493.

Beillas P, Lavaste F, Nicoloupoulos D, Kayventash K, Yang KH, Robin S. (1999) Foot and ankle finite element modeling using CT-scan data. Stapp Car Crash Conference Proceedings, pp. 1–14.

Bennett, MB, Ker RF. (1990) The mechanical properties of the human subcalcaneal fat pad in compression. *Journal of Anatomy*, Vol. 171, pp. 131–138.

Bose D, Bhalla K, Rooij L, Millington S, Studley A, Crandall J. (2004) Response of the Knee joint to the pedestrian impact loading environment. SAE World Congress, paper 2004-01-1608.

Burstein AH, Currey JD, Frankel VH, Reilly DT. (1972) The ultimate properties of bone tissue: the effects of yielding. *Journal of Biomechanics*, Vol. 8, No. 6, pp. 393–396.

Crandall JR, Portier L, Petit P, Hall GW, Bass CR, Klopp GS, Hurwitz S, Pilkey WD, Trosseille X, Tarriere C, Lassau JP. (1996) Biomechanical response and physical properties of the leg, foot, and ankle. 40th Stapp Car Crash Conference Proc. SAE, pp. 173–192.

Dhaliwal TS, Beillas P, Chou CC, Prasad P, Yang KH, King AI. (2002) Structural response of lower leg muscles in compression: A low impact energy study employing volunteers, cadavers and the hybrid III. *Stapp Car Crash Journal*, Vol. 46, pp. 229–243.

Goldstein SA. (1987) The mechanical properties of trabecular bone: Dependence on anatomic location and function. *Journal of Biomechanics*, Vol. 20, No. 11.12, pp. 1055–1061.

Haut RC, Atkinson PJ. (1995) Insult to the human cadaver patellofemoral joint: Effect of age on fracture tolerence and occult injury. 39th Stapp Car Crash Conference Proceedings, no. 952729, SAE, pp. 281–294.

Hayashi S, Choi HY, Levine RS, Yang KH, King AI. (1996) Experimental and analytical study of knee fracture mechanisms in a frontal knee impact. 40th Stapp Car Crash Conference Proceedings, pp. 161–171.

IHRA/PS/200 (2001) International Harmonized Research Activities. *Pedestrian Safety Working Group Report*. Available at: http://www-nrd.nhtsa.dot.gov/ihra/Pedestrian/pedestrian.html

Johnson GA. (1996) A single integral finite strain viscoelastic model of ligaments and tendons. *Journal of Biomechanical Engineering*, Vol. 118, pp. 221–226.

Kajzer J, Cavallero C, Bonnoit J, Morjane A, Ghanouchi S. (1990) Response of the knee joint in lateral impact: Effect of shearing loads. Proc. IRCOBI, pp. 293–304.

Kajzer J, Cavallero C, Bonnoit J, Morjane A, Ghanouchi S. (1993) Response of the knee joint in lateral impact: Effect of bending moment. Proc. IRCOBI, pp. 105–116.

Kennedy JC, Weinberg HW, Wilson AS. (1974) the anatomiey and function of the anterior cruciate ligament. *Journal of Bone and Joint Surgery*, Vol. 56, pp. 223–235.

Kerrigan JR, Ivarsson BJ, Bose D, Madeley NJ, Millington SA, Bhalla KS, Crandall JR. (2003) Rate sensitive constitutive and failure properties of human collateral knee ligaments. IRCOBI Conference, pp. 177–192.

Li LP, Buschmann MD, Shirazi-Adl A. (2003) Stain rate depedent stiffness of articular cartilage in unconfined compression. *Journal of Biomechanical Engineering*, Vol. 125, pp. 161–168.

Lizee E, Robin S, Soong E, Bertholon N, Le Coz JY, Besnault B, Lavaste F. (1998) Developpement of a 3D finite element model of the human body. SAE no. 983152. Proc. Stapp Car Crash Conf., pp. 215–238.

Marinozzi G, Pappalardo S, Steindler R. (1982) Human knee ligaments: Mechanical tests and ultrastructural obseravtions. *Italian Journal of Orthopaedic and Trauma*, Vol. 9, pp. 231–240.

McElhaney JH. (1966) Dynamic response of bone and muscle tissue. *Journal of Applied Physiology*, Vol. 21, No. 4, pp. 1231–1236.

Mow VC, Kuei SC, Lai WM, Holmes MH. (1980) Biphasic creep and stress relaxation of articular cartilage in compression. Theory and experiment. *Journal of Biomechanical Engineering*, Vol. 102, pp. 73–84.

Noyes FR. (1976) The strength of the anterior cruciate ligament in humans and rhesus monkeys. *Journal of Bone and Joint Surgery*, pp. 1074–1081.

Nyquist GW, Cheng R, El-Bohy AR, King AI. (1985) Tibia bending: Strength and response. 29th Stapp Car Crash Conference Proc., no. 851728, pp. 99–112.

Parenteau CS. (1996) Foot and Ankle joint response—epidemiology, biomechanics and mathematical modelling. PhD dissertation, Chalmers University, Göteborg, Sweden.

Prietto MP, Bain JR, Stonebrook SN, Settleage RA. (1992) Tensile strength of the human posterior cruciate ligament (PCL). *Transactions of the Orthopaedic Research Society*, Vol. 17, p. 124.

Race A. (1976) The mechanical properties of the two bundles of the human posterior cruciate ligament. *Journal of Biomechanics*, Vol. 9, pp. 449–452.

Radin EL, Paul IL, Lowy M. (1970) A comparison of the dynamic force transmitting properties in subchondral bone and articular cartilage. *Journal of Bone and Joint Surgery*, Vol. 52A, pp. 444–456.

Reilly DT, Burstein AH. (1975) The elastic and ultimate properties of compact bone tissue. *Journal of Biomechanics*, p. 393.

Repo R, Finlay J. (1977) Survival of articular cartilage after controlled impact. *Journal of Bone and Joint Surgery*, Vol. 59, p. 1068.

Schuster PJ, Chou CC., Prasad P, Jayaraman G. (2000) Development and Validation of a Pedestrian Lower Limb Non-Linear 3-D Finite Element Model. 44th Stapp Car Crash Conference Proceedings. Atlanta, 2000-01-SC21.

Stutts JC, Hunter WW. (1999) Motor vehicle and roadway factors in pedestrian and bicyclists injuries: An examination based on emergency department data. *Accident Analysis and Prevention*, Vol. 31, No. 5, pp. 505–514.

Tannous RE, Bandak FA, Toridis TG, Eppinger RH. (1996) A three-dimensional finite element model of the human ankle: Development and preliminary application to axial impulsive loading, 40th Stapp Car Crash Conference Proc, SAE. pp. 219–238.

Takahashi Y, Kikuchi Y, Mori F, Konosu A. (2003) Advanced FE lower limb model for pedestrians. International Technical Conference on the Enhanced Safety of Vehicles, Nagoya, Japan. Paper no. 218.

Teresinski G, Madro R. (2001) Pelvis and hip injuries as a reconstructive factors in car-to-pedestrian accidents. *Forensic Science International*, Vol. 124, pp. 68–73.

Thollon L. (2001) Modélisation du membre thoracique dans le cadre d'un choc latéral: Approche expérimentale et numérique. PhD dissertation. Université de la Méditerranée, Marseilles, France.

Thollon L, Arnoux PJ, Kayvantash K, Cavallero C, Brunet C. (2002) From dummy criteria to injury evaluation using Humos Radioss finite element model. Proceedings of the IRCOBI conference, Munich, pp. 369–373.

Tropiano P, Thollon L, Arnoux PJ, Behr M, Kayvantash K, Brunet C. (2004) Finite element analysis and virtual traumatology: Application to Neck-injury in frontal crash situations. *Spine*, Vol. 29, No. 16, pp. 1709–1716.

Viano DC, Culver CC, Haut RC, Melvin JW, Bender M, Culver RH, Levine RS. (1978) Bolster impacts to the knee and tibia of human cadavers and an anthropomorphic dummy. 22nd Stapp Car Crash Conference Proc., p. 401.

Viidick A. (1973) Functional properties of collagenous tissues. *International Review of Connective Tissue Research*, Vol. 6, Academic Press, New York.

Yamada H. (1970) *Strength of biological materials*. Ed. F. Gaynor Evans.

Yang J. (1997) Injury biomechanics in car pedestrian collisions: Development, validation and application of Human-Body mathematical models. PhD dissertation. Chalmers University, Göteborg, Sweden.